Available online at www.sciencedirect.com
ScienceDirect
Ceramics International 34 (2008) 581–591
CERAMICS INTERNATIONAL
www.elsevier.com/locate/ceramint

Evaluation of aluminum dross waste as raw material for refractories

H.N. Yoshimura *, A.P. Abreu, A.L. Molisani, A.C. de Camargo, J.C.S. Portela, N.E. Narita

Laboratory of Metallurgy and Ceramic Materials, Institute for Technological Research of the State of São Paulo, Av. Prof. Almeida Prado, 532, São Paulo, SP 05508-901, Brazil

Received 16 January 2006; received in revised form 19 March 2006; accepted 18 December 2006
Available online 30 January 2007

Abstract

An aluminum dross waste from plasma processing for Al metal reclamation was tested as a replacement raw material in refractories. The main phases of the starting Al dross waste material were $MgAl_2O_4$ and AlN. The waste was tested to replace calcined alumina in castables and refractory clay in a molded refractory at levels below 6.5%. The results of physical and mechanical tests indicated that the waste may be applied directly, without prior calcination, as a substitute for fine structural components in refractories. The waste and water contents used in processing, however, must be optimized to avoid the formation of crack-like defects in the microstructure. The origin of these defects is related to the generation of gas from the waste at high temperatures. It is not known if these crack defects impact physical properties. The waste was also tested as a replacement for anti-oxidant elements (Al and Si powders) in a resin-bonded refractory. Oxidation tests, however, indicated a negative effect on oxidation resistance.

© 2007 Elsevier Ltd and Techna Group S.r.l. All rights reserved.

Keywords: B. Microstructure-final; C. Strength; E. Refractories; Recycling

1. Introduction

Aluminum dross is formed on the surface of molten Al that is exposed to furnace atmosphere during primary and secondary Al fusion processing. The Al dross usually is a mixture of free Al metal and nonmetallic substances, like aluminum oxide, nitride, and carbide; salts; and metal oxides. The overall chemistry depends on the alloying elements present in the molten Al and the metallurgical practices [1].

The traditional technique to recover metallic Al involves heating the dross in a rotating furnace using a salt flux (usually an eutectic mixture of NaCl and KCl with small amount of cryolite or CaF_2), which helps in the separation of molten Al from the solid oxide fraction and protects the Al metal against oxidation [2,3]. The waste of this process, however, contains large amounts of water-leachable salts that contaminate the environment when disposed of in landfills. Other elements and compounds may also have deleterious effects on the environment, like Pb, and the non-recovered metallic Al, Al_4C_3, and AlN; which can degrade and react with water to produce hydrogen, methane, and ammonia gases, respectively [4]. Millions of tonnes of Al dross waste have been discarded in landfills annually worldwide, including in Brazil, one of the world's largest aluminum producers and recyclers [5].

Some methods have been proposed to recycle the salt containing Al dross waste so that it can be used to prepare raw materials or ceramic products. Calcining dry compacts of Al dross waste in a direct fired rotary kiln above 982 °C results in a refractory product containing mainly spinel ($MgAl_2O_4$) and corundum (α-Al_2O_3); which has a high refractoriness (pyrometric cone equivalent above 37 or 1821 °C) [6]. After leaching to remove the water soluble salts, the waste can be mixed with inorganic additives and melted to form a silicate-based glass that is poured to form fibers or abrasive particles [7]. Washed Al dross waste containing $MgAl_2O_4$, AlN, quartz (SiO_2), Al, α-Al_2O_3, periclase (MgO), and $Al(OH)_3$ can be used to prepare a $(Mg,Si)Al_2O_4$ spinel by induction synthesis [4]. Furthermore, washing with hot water transforms AlN to $Al(OH)_3$ and removes Na and K chlorides from the waste [4].

Another way to recover Al from Al dross is in the use a plasma arc torch as a heating source [8,9]. The plasma treatment of Al dross is a promising technique [10] among the proposed salt-free Al dross treatment processes [11]. Nowadays there are two plasma processing plants of Al dross: the Alcan

* Corresponding author. Tel.: +55 11 3767 4549; fax: +55 11 3767 4037.
E-mail address: hnyoshim@ipt.br (H.N. Yoshimura).

0272-8842/$34.00 © 2007 Elsevier Ltd and Techna Group S.r.l. All rights reserved.
doi:10.1016/j.ceramint.2006.12.007

plant in Canada and the Plasma Processing Corp. plant in USA, with annual capacities of 14,000 and 40,000 t, respectively [12]. Salt flux is not used to recover the metal in this technique, therefore the waste has no environmental problems caused by soluble salts of dross treated in the traditional way. However, the Al dross waste from plasma processing still contains appreciable amounts of AlN, and may still be unsuitable for disposal in landfill sites since this chemical is considered a pollutant [13]. A reported composition range of this waste indicates the presence of 50–65 wt% Al_2O_3 (including the fraction as spinel); 15–30 wt% AlN; 3–5 wt% Al; 5–10 wt% MgO; 1–2 wt% SiO_2; <2 wt% CaF_2; and <2 wt% NaF [14]. Some methods have also been proposed to prepare refractory aggregates using the plasma-processed waste. It has been suggested that the heat generated by the exothermic oxidation reaction of AlN during calcination of waste dross mixed with metal oxides can favor the formation of refractory compounds like spinel, mullite, sialon, and calcium aluminates [13,14].

The interest to investigate the use of Al dross waste as refractory aggregate is related mainly to the high Al_2O_3 contents of these materials. Alumina is the primary ingredient for a significant portion of the refractory products used in high-temperature industrial applications; like metallurgical, cement, ceramic, glass, and petrochemical manufacturing process [15]. The total world consumptions of calcined refractory-grade bauxite and calcined aluminas for use in refractory applications are ~1 million and ~500,000 metric tonnes per year, respectively [15,16]. There is also some market potential for use of Al dross waste as an alternative Al_2O_3 source for refractory aggregates.

Although there are proposals to produce refractory aggregates from Al dross wastes, few techniques have shown the performance of the refractories prepared with these materials. Park et al. [17] used a waste dross calcined at 900 °C to replace the cement or small aggregate (<0.074 mm) of a castable and observed that compressive and bending strengths were in general above the minimum values required for the application. The results also showed that the values of these properties decreased with increasing waste content (5–30 wt%). No explanation, however, was presented for the deleterious effect of the waste in the castable.

In general, the methods proposed to apply the Al dross waste as refractory aggregates involve high temperature heat treatments. These methods, however, are expensive and limit the reclamation of Al dross waste. The aim of this work was to investigate the possibility of direct refractory use, without prior calcination, of an Al dross waste from plasma processing as raw material in castables and pressed brick.

2. Experimental

The Al dross waste used in this work was a by-product of experimental runs for recovering Al metal from Al dross generated by a Brazilian primary Al factory. A pilot scale plasma arc torch heated furnace developed by Dr. Antonio Carlos da Cruz (Laboratory of Plasma, Institute for Technological Research of the State of São Paulo) was used to recover the metal. The Al dross waste from plasma processing was first deagglomerated by dry ball milling for 1 h and then screened to remove agglomerates larger than 1 mm. Among these agglomerates, large metal-like pieces, probably metallic Al, were observed. The >1 mm waste returned for plasma processing to recover the Al metal. The remaining powder (84 wt% of the original mass) was directly used for replacement of raw materials in refractories. Previous investigation [18] indicated that this powder could have high quantities of refractory compounds (Al_2O_3, $MgAl_2O_4$, AlN) and a low content of fluxing oxides (SiO_2, CaO, Na_2O, K_2O) and Al metal. The possible high refractoriness of <1 mm powder indicated that the Al dross waste could be applied as a substitute for fine components (calcined alumina and refractory clay) in castables and pressed bricks. Another possible application could be the use of Al dross waste as a substitute for anti-oxidant elements (Al and Si powders) in carbon-containing refractories, since non-oxide compounds like AlN could protect the refractory against oxidation.

Table 1
Basic compositions (wt%) of low-cement castable (LCC), ultra-low-cement castable (ULCC), and self-flowing castable (SFC)

Component	LCC	ULCC	SFC
White fused alumina 5/16/4	0	26	15
White fused alumina 4/10	33	16	13
White fused alumina 8/20	21	14	15
White fused alumina 20/40	4	10	0
White fused alumina 100 mesh (TPF)	10	5	19.5
White fused alumina 325 mesh (TPF II)	19	22	20
Calcined alumina	5	3	6.5
Refractory clay	0	0	1
Silica fume	5	3	5
Hydraulic cement	3	1	5
Sodium tripolyphosphate	0.1[a]	0.03[a]	0.1[a]

[a] wt% over total mass.

Three types of castable refractories were investigated with/without dross: low-cement castable (LCC), ultra-low-cement castable (ULCC), and self-flowing castable (SFC). The basic compositions of these castables are shown in Table 1. In these compositions, the percent of calcined alumina was replaced by Al dross waste on a 0 (control), 50, and 100% level. The actual contents of Al dross waste added to the castables are shown in Table 2. The procedure used for castable preparation followed the Brazilian standard (ABNT NBR 8382). Using this standard, dry raw materials (3 kg per batch) were mixed in a planetary mixer and, after the addition of the required amount of water to achieve the proper consistency (Table 3), the mix was poured into a metallic mold with three cavities (40 mm × 40 mm × 160 mm). For LCC and ULCC samples, the mold was filled by mechanical vibration; while for SFC samples, molds were filled by self-flowing properties of the mix. All specimens were stored in a humid chamber (27 °C; 80% relative humidity) for 24 h and then exposed in room air for at least 24 h. During the storage of Al dross waste containing specimens; AlN phase could have reacted with added water, forming NH_4OH gas. The ammonia smell, however, was not noticed during the storage, indicating limited reaction

Table 2
Al dross waste content added to low-cement castable (LCC), ultra-low-cement castable (ULCC), self-flowing castable (SFC), and pressed (P) samples

Castable	Al dross content (wt%)		
	0	50%	100%
LCC	0	2.5	5.0
ULCC	0	1.5	3.0
SFC	0	3.2	6.5
P	0	1.5	3.0

Table 3
Water content used for preparation of low-cement castable (LCC), ultra-low-cement castable (ULCC), and self-flowing castable (SFC) samples

Castable	Water content (wt%)		
	0	50%	100%
LCC	5.2	5.7	6.0
ULCC	4.0	4.3	4.5
SFC	6.7	7.0	7.7

extension. After drying at 110 °C for 24 h, the specimens were fired in an electric furnace at 815 or 1450 °C for 5 h using a heating rate of 5 °C/min.

Two types of molded refractories were investigated: pressed (P) and resin-bonded (R). The basic compositions of these refractories are shown in Table 4. In P refractory compositions, the percent of refractory clay was replaced by Al dross waste at 0 (control), 50, and 100% level. The actual content of dross waste added to pressed samples is shown in Table 2. In the R refractory composition, the Al dross waste replaced the anti-oxidant metallic powders (Al and Si). Two control samples were prepared: R0, without metallic powder and waste; and RAS, with 3.5 wt% Al and 2 wt% Si. Two samples with Al dross waste additions were prepared: RWS, with 3.5 wt% waste substituting for Al powder and 2 wt% Si; and RW, with 5.5 wt% waste as a replacement for both the Al and Si powders. Molded refractory specimens (50 mm in diameter and 50 mm in height) were prepared by manual mixing raw materials with 1% distilled water, pressing at 150 MPa in cylindrical die, drying (at 110 °C for at least 24 h for P samples and at 190 °C for 9 h for R samples) and; for P samples, firing in an electric furnace at 1450 °C for 5 h using a heating rate of 5 °C/min.

Table 4
Basic compositions (wt%) of pressed refractory (P) and resin-bonded refractory (R)

Component	P	R
White fused alumina 4/10 mesh	18	30
White fused alumina 8/20 mesh	23	20
White fused alumina 20/40 mesh	28	8
White fused alumina 100 mesh (TPF)	0	16
White fused alumina 325 mesh (TPF II)	26	6.5
Calcined alumina	0	7
Refractory clay	3	0
Quartz 325 mesh	2	0
Organic binder	0.5[a]	0
Magnesium lignosulfate	3[a]	0
Aluminum powder	0	3.5
Silicon powder	0	2
Graphite	0	7
Phenolic resin	0	3.3[a]

[a] wt% over total mass.

The starting materials were characterized by chemical analysis, X-ray diffraction (XRD), specific surface area (BET method), particle size distribution (laser diffraction method), refractoriness (pyrometric cone equivalent), scanning electron microscopy (SEM), and energy dispersive spectroscopy (EDS).

Dried and fired refractory samples were analyzed using three-point bending and compression tests (at room temperature), linear change, bulk density and apparent porosity (Archimedean's method with water as the immersion liquid), and stereo-optical microscopy.

For evaluation of the oxidation resistance of resin-bonded refractories, dried specimens were heat-treated at 1250 and 1450 °C for 0.5–5 h in air using an electric furnace. Fired cylindrical specimens were cut with a diamond saw at mid-height and the cross-section of specimen analyzed using an image analyzer in order to measure the non-decarburized area (dark central region). The images used in this analysis were captured directly with a digital camera (macroanalysis) from the cross-sections of specimens (50 mm in diameter). The decarburized and non-decarburized areas were clearly distinguishable by naked eye. The thickness of oxidation layer was calculated by subtracting the equivalent radius of this area from the radius of the specimen cross-section.

The statistical analysis of the results was made by means of Student's *t*-test method at 95% confidence interval.

3. Results and discussion

3.1. Dross characterization

The main crystalline phases identified in raw Al dross waste were spinel ($MgAl_2O_4$) and aluminum nitride (AlN), with small amounts of corundum (α-Al_2O_3), aluminum oxynitride

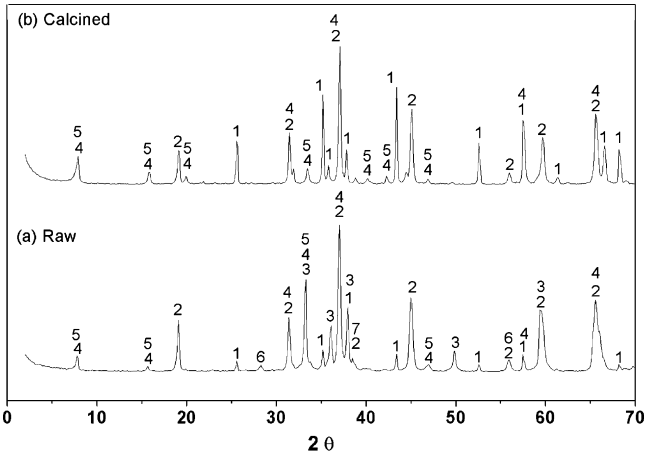

Fig. 1. X-ray diffraction patterns of (a) raw and (b) calcined Al dross waste. *Key*: (1) α-Al_2O_3; (2) $MgAl_2O_4$; (3) AlN; (4) $(NO)_2Al_{22}O_{34}$; (5) $NaAl_{11}O_{17}$; (6) CaF_2; (7) Al metal.

Table 5
Crystalline phase contents (wt%) evaluated by semi-quantitative XRD analysis of raw Al dross waste

$MgAl_2O_4$	48
AlN	28
α-Al_2O_3	7
$(NO)_2Al_{22}O_{34}$	6
$NaAl_{11}O_{17}$	6
CaF_2	3
Al	2

Table 6
Results (wt%) of chemical analysis of raw Al dross waste

Al	47.2
Mg	7.6
F	2.0
Na	1.0
Si	0.89
K	0.73
Ca	0.73
Fe	0.23
Zr	0.14
Ti	0.12

$[(NO)_2Al_{22}O_{34}]$, β-Al_2O_3 ($NaAl_{11}O_{17}$), calcium fluoride (CaF_2), and metallic Al (Fig. 1a, Table 5). The chemical analysis of raw Al dross waste indicated a high content of Al and Mg and small amounts of F, Na, Si, K, Ca, Fe, Zr, and Ti (Table 6). Traces of S, Mn, Ni, Cu, Zn, P, Ga, Sr, Sn, Co, and Cr were also detected. In order to evaluate the equivalent oxide content of metallic elements, the waste was calcined at 1450 °C for 1 h in air. Calcination resulted in oxidation of phases like AlN, metallic Al, and CaF_2. The calcined Al dross waste consisted mainly of corundum and spinel phases, with small amounts of β-Al_2O_3 and aluminum oxynitride phases (Fig. 1b). Chemical analysis of calcined waste indicated 84 wt% Al_2O_3, 11 wt% MgO, and 5 wt% impurities (Table 7). The dross impurities can form low melting point phases, including SiO_2, CaO, Na_2O, K_2O, Fe_2O_3, and TiO_2. Most of the nitrogen (mainly from AlN), fluorine, and sulfur were lost during the calcination. Considering all MgO as $MgAl_2O_4$ (as indicated by XRD results in Fig. 1b), the mass fraction of stoichiometric spinel in the calcined waste was ~50%. The remaining material was ~45 wt% α-Al_2O_3 and ~5 wt% β-Al_2O_3, aluminum oxynitride, with a possible silicate-based glassy phase forming from the impurities. The mass of the waste dross increased 6.0% after calcination at 1450 °C, mainly because of the oxidation of AlN compound. The expected mass variations from oxidation of AlN to Al_2O_3, Al to Al_2O_3, and CaF_2 to CaO are +24.4, +88.9, and −28.2%, respectively.

Table 7
Results (wt%) of chemical analysis of Al dross waste calcined at 1450 °C for 1 h in air

Al_2O_3	84
MgO	11
SiO_2	2
CaO	1
Na_2O	0.7
K_2O	0.4
Fe_2O_3	0.3
TiO_2	0.3

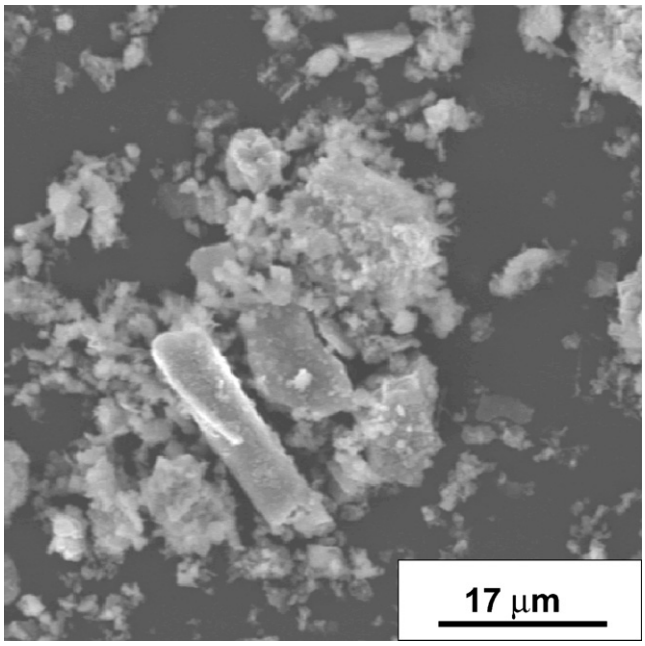

Fig. 2. SEM image of Al dross waste.

The Al dross waste was a mixture of fine particles with large agglomerated particles (Fig. 2). The average particle size and specific surface area were 26.3 μm and 4 m^2/g, respectively. The as received dross had a high refractoriness, above 1743 °C (Orton cone 33), since it was composed mainly of high melting point phases.

3.2. Refractory sample characterization

The water content needed to prepare castable refractory samples increased slightly with the increase of Al dross waste fraction in the three types of castable investigated (LCC, ULCC,

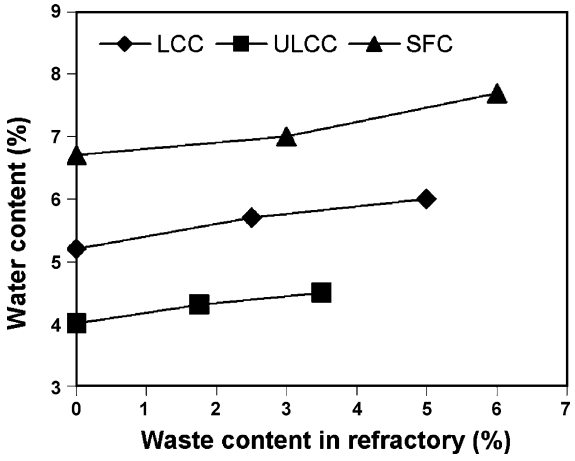

Fig. 3. Water content used to prepare samples of low-cement (LCC), ultra-low-cement (ULCC), and self-flowing (SFC) castables as a function of Al dross waste content in refractory.

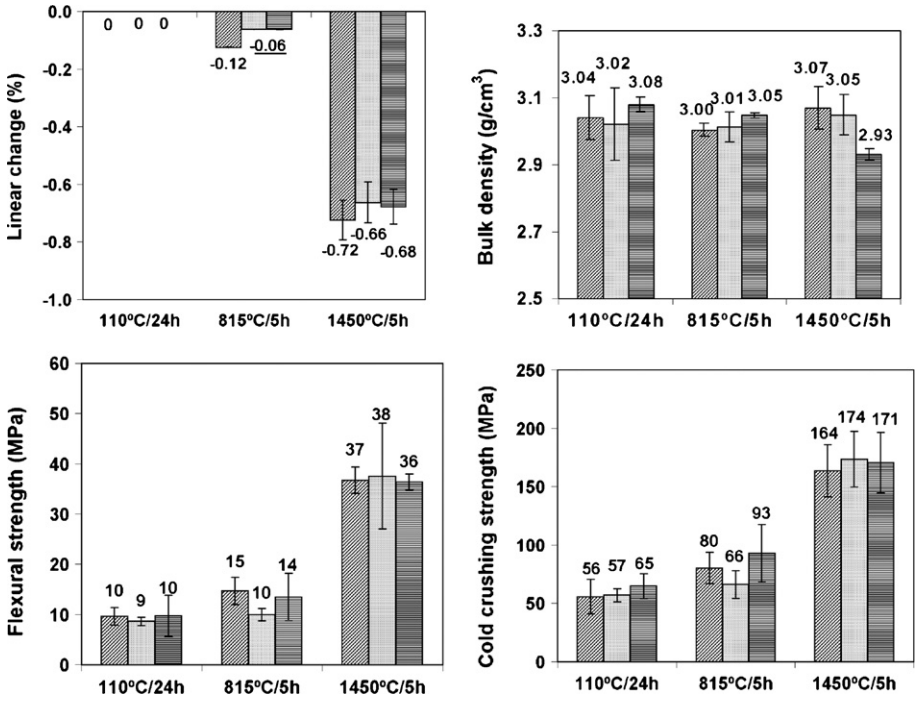

Fig. 4. Results of linear change, bulk density, flexural strength at room temperature, and cold crushing strength of low-cement castable samples (LCC) after drying at 110 °C and firing at 815 and 1450 °C with 5% calcined alumina replaced by varying Al dross waste levels. Underlined value is statistically different from the value of control sample (at 95% confidence interval). Fraction of waste replacing 5% calcined alumina: (▨) 0%; (▢) 50%; (▤) 100%.

and SFC, Fig. 3). Probably this occurred because a fraction of added water was consumed by the reaction with AlN to form NH_4OH, although no ammonia smell was noticed. Note that in a preliminary experiment, a refractory mortar was prepared using only the waste dross as aggregate. This material was difficult to process because of the strong smell caused by large amount of ammonia gas that evolved. It is possible that NH_4OH generated by the dross could have changed the castable pH during mixing of

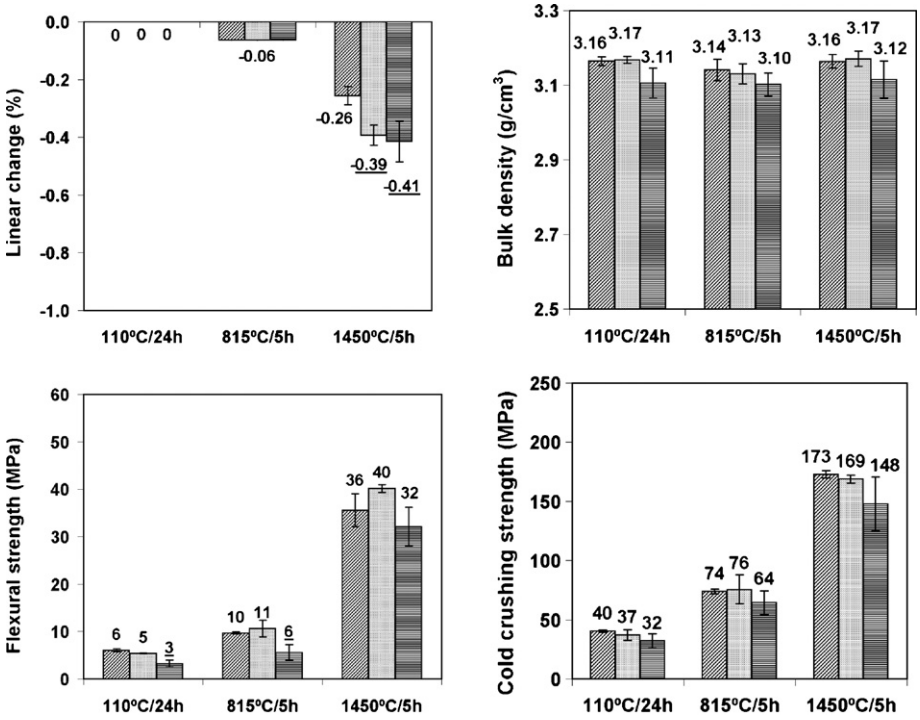

Fig. 5. Results of linear change, bulk density, flexural strength at room temperature, and cold crushing strength of ultra-low-cement castable samples (ULCC) after drying at 110 °C and firing at 815 and 1450 °C with 3% calcined alumina replaced by varying Al dross waste levels. Underlined value is statistically different from the value of control sample (at 95% confidence interval). Fraction of waste replacing 3% calcined alumina: (▨) 0%; (▢) 50%; (▤) 100%.

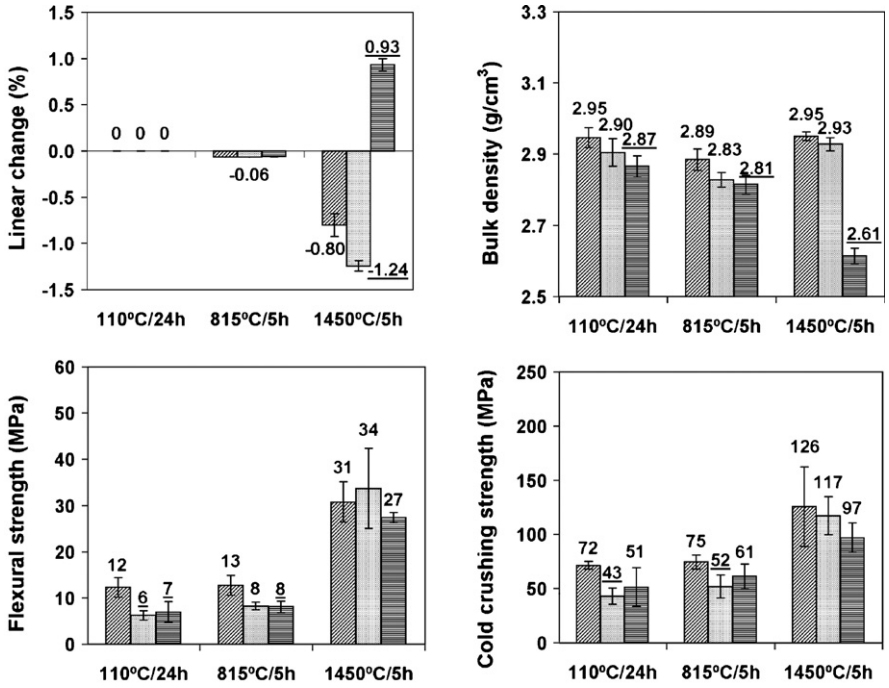

Fig. 6. Results of linear change, bulk density, flexural strength at room temperature, and cold crushing strength of self-flowing castable samples (SFC) after drying at 110 °C and firing at 815 and 1450 °C with 6.5% calcined alumina replaced by varying Al dross waste levels. Underlined value is statistically different from the value of control sample (at 95% confidence interval). Fraction of waste replacing 6.5% calcined alumina: (▨) 0%; (▥) 50%; (▤) 100%.

the refractory components, and diminishing the flowability of alumina aggregates. This pH change can impact the water content needed to prepare dross containing catables. The possible effects of ammonia gas evolution and water content on castable porosity will be discussed later.

3.2.1. Physical properties

Physical property results measured on the LCC, ULCC, and SFC castables and P refractories are shown in Figs. 4–7. The error bars shown represent ±1 standard deviation calculated from at least three measurements (specimens). The main observations related to the samples with the additions of Al dross waste are:

(i) for LCC castables (Fig. 4), most of the results of samples with the additions of Al dross waste were statistically similar to the control sample (at 95% confidence interval), except the significant lower values of shrinkage (linear change) of the samples with 50 and 100% dross waste replacing calcined alumina fired at 815 °C;

(ii) for ULCC castables (Fig. 5), most of the results of samples with the additions of Al dross waste were also statistically similar to the control sample (at 95% confidence interval). An exception was the significant higher values of shrinkage of the samples with dross waste fired at 1450 °C, but they were low (∼0.4%) and acceptable for a castable. The sample with 100% dross waste replacing calcined alumina presented significant lower values of flexural strength after drying at 110 °C and firing at 815 °C than the control sample, however, it presented statistically similar values of this property after firing at 1450 °C, in relation to the control sample;

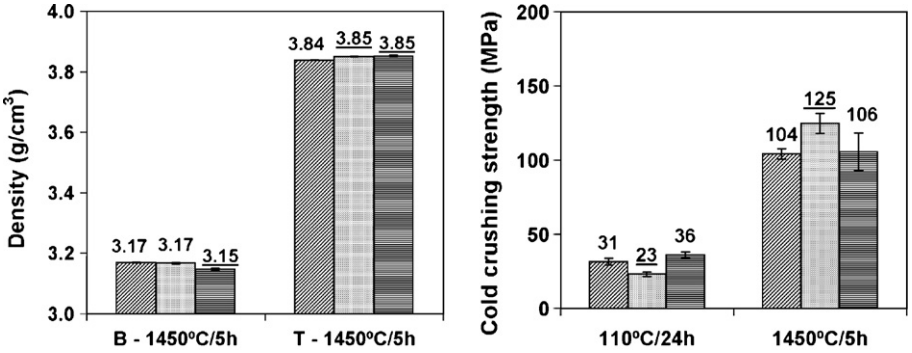

Fig. 7. Results of pressed refractories (P): bulk density, *B*, and apparent solid density, *T*, after firing at 1450 °C; and cold crushing strength after drying at 110 °C and firing at 1450 °C with 3% refractory clay replaced by varying Al dross waste levels. Underlined value is statistically different from the value of control sample (at 95% confidence interval). Fraction of waste replacing 3% refractory clay: (▨) 0%; (▥) 50%; (▤) 100%.

(iii) for SFC castables (Fig. 6), many values of measured properties of the samples with dross waste were statistically different than the control sample (at 95% confidence interval). The sample with 50% dross waste replacing calcined alumina had a significantly higher value of shrinkage, after firing at 1450 °C; a lower value of flexural strength, after drying at 110 °C; and a lower cold crushing strength, after drying at 110 °C and firing at 815 °C, in relation to the control sample. The results of mechanical strengths of this sample, however, were similar to the control sample after firing at 1450 °C. The sample with 100% dross waste replacing calcined alumina presented, after firing at 1450 °C, significant expansion and low bulk density. This sample also presented significant lower values of bulk density and flexural strength, after drying at 110 °C and firing at 815 °C; the flexural strength, however, was similar to the control sample after firing at 1450 °C. Although the firing at 1450 °C caused the expansion of this sample, the mechanical properties at room temperature were not impacted significantly by the significant decreasing of bulk density;

(iv) for pressed refractories (Fig. 7), the sample with 100% dross waste replacing refractory clay had significantly lower values of bulk density and both samples with Al dross waste had significant higher values of apparent solid density, after firing at 1450 °C, compared to the control sample. The differences, however, were low (less than 1%) and not considered relevant. The sample with 50% dross waste replacing refractory clay presented significantly lower value of cold crushing strength after drying at 110 °C, however, it had significantly higher value of this property after firing at 1450 °C, in relation to the control sample. The remaining results of the samples with Al dross waste were statistically similar to the control sample (at 95% confidence interval);

(v) all investigated samples of castable and pressed refractories had results of physical and mechanical properties similar to or better than the industrial products, with the exception for the expansion observed in SFC castable with 100% waste replacing calcined alumina that was fired at 1450 °C.

3.2.2. Microstructure

Refractory samples presented similar general microstructural features when compared at the same condition of drying or firing temperature. Some spherical macropores with size up to 2 mm were observed in all castable samples (with and without waste). No significant difference was observed among the microstructures of the samples with Al dross and the control samples after drying at 110 °C, on the optical microscopy level. This result indicated that the possible ammonia gas generated by the dross and the slightly higher water content needed to process the samples with Al dross waste (Fig. 3) had little effect on the castable porosity. The similar results of bulk density among the 110 °C dried samples, with and without dross (Figs. 4–6), support this observation. Even for the SFC sample with 100% dross waste replacing calcined alumina, which presented significant lower value of bulk density after drying at 110 °C (Fig. 6), had a small difference in bulk density compared to the control sample (2.7%), a difference which did not impact significantly the microstructure of this sample after drying at 110 °C.

Small microstructural modifications were observed in samples fired at 815 °C in relation to the samples dried at 110 °C, with significant changes observed in the samples fired at 1450 °C. The samples fired at 1450 °C had a more compact structure. This change can be observed comparing the optical micrographs of LCC sample fired at 815 °C (Fig. 8a) and at 1450 °C (Fig. 8b). Some castable samples with Al dross waste contained pore-like defects after firing at 1450 °C. The LCC sample with 100% dross waste and SFC samples with 50 and 100% dross waste (dross replacing calcined alumina), presented long crack-like defects (Fig. 8c). The SFC sample with 100% dross waste also contained many pores in the microstructure (Fig. 8e). These defects were not observed in the same samples after drying or firing at 815 °C, showing that they were formed after firing at high temperature (1450 °C). All ULCC and pressed refractory samples did not present these types of defects, even after firing at 1450 °C (Fig. 8d and f). The morphologies of the defects and the expansion of SFC sample with 100% dross waste (Fig. 6) suggested that the defects were caused by gas evolution at high temperature.

Some reactions that can occur with the evolution of gas in the samples containing the waste are: (i) reaction of AlN with water forming Al hydroxide and ammonia gas; (ii) reaction of metallic Al with water to form Al hydroxide and hydrogen gas; (iii) dehydration of Al hydroxides forming transition aluminas and water vapor; (iv) oxidation of CaF_2 to form CaO and fluorine containing gas; and (v) oxidation of AlN, and possibly oxynitrides, forming alumina and nitrogen gas [19–23]. The hydrolysis of AlN and metallic Al results in the formation of bayerite—$Al(OH)_3$ [19,20], which on heating, decomposes to boehmite (AlOOH) at ~100 °C and then to γ-Al_2O_3 at ~500 °C [21]. Therefore, the first three reactions (i, ii, and iii) are expected to occur at low temperatures (below ~600 °C). Since the defects were formed at high temperature (above 815 °C), the last two reactions could have caused the formation of the defects.

Green strength and the ability to handle and store green materials before firing are important in the commercial production of a material. The green strength of the studied refractories, however, was not evaluated. No additional difficulty in to handle the specimens with Al dross waste during the processing of these materials was observed in relation to the control specimens. So, it is expected that the green strength and the ability to handle materials will not be significantly affected by the addition of Al dross waste in the refractories. A specific study, however, is necessary to confirm this hypothesis.

3.2.3. Porosity and oxidation resistance

Porosity is an important feature of a refractory material, since it can affect the thermo-mechanical behavior and the

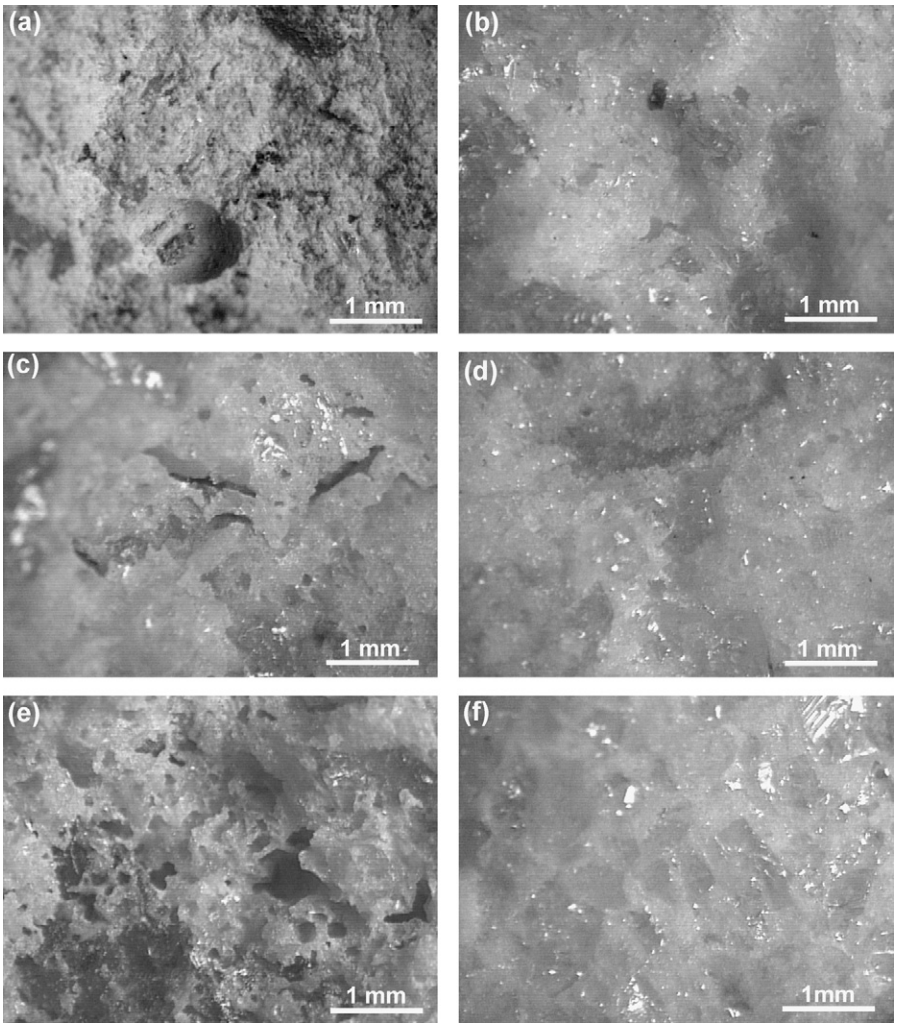

Fig. 8. Optical micrographs of refractory samples: (a) LCC-100% fired at 815 °C; (b) LCC-50% fired at 1450 °C; (c) LCC-100% fired at 1450 °C; (d) ULCC-100% fired at 1450 °C; (e) SFC-100% fired at 1450 °C; and (f) P-100% fired at 1450 °C. The percentages indicate the fraction of Al dross waste replacing calcined alumina, CA, in castable samples (LCC-5% CA, ULCC-3% CA, and SFC-6.5% CA) and refractory clay (RC) in pressed sample (P-3% RC).

performance in use, of properties such as the mechanical strength, thermal shock resistance, gas permeability, and resistance against attack by molten metal and slag. Pore size, shape, fraction, and distribution are some relevant characteristics of the porosity, but they were not evaluated in this work.

The effect of Al dross waste addition on total porosity, however, can be inferred from the results of bulk density. Two trends were observed from the results: (i) porosity affected by the processing, which can be analyzed from the results of bulk density after drying at 110 °C and firing at low temperature (815 °C); and (ii) porosity generated at high firing temperature (1450 °C). In the first trend, only the SFC sample with 100% Al dross waste replacing calcined alumina presented statistically significant lower values of bulk density after drying at 110 °C and firing at 815 °C versus control sample (without dross). This change correlated to the significant lower values of flexural strength after drying at 110 °C and firing at 815 °C (Fig. 6). The sample prepared with the highest fraction of Al dross waste (6.0%) and the highest content of water (7.7%, Fig. 3), had a significant decrease in bulk density (increasing of porosity). The significantly lower values of flexural strength after drying at 110 °C and cold crushing strength after drying at 110 °C and firing at 815 °C of the SFC sample with 50% Al dross waste replacing calcined alumina can also be related to the lower average values of bulk density, although they were not statistically different compared to the results of control sample (at 95% confidence interval, Fig. 6). Similar correlations (with the lower average values of bulk density) seems to explain the significant lower values of flexural strength of the ULCC sample with 100% Al dross waste replacing calcined alumina after drying at 110 °C and firing at 815 °C (Fig. 5). These results indicate that the addition of Al dross waste impacts the porosity of castables, but not at a level that precludes its use in refractory materials, at least related to mechanical properties. The effects of dross additions, however, must be evaluated in specific properties, like slag resistance, before considering other applications.

Concerning the second trend, porosity generated at high firing temperature, only the SFC sample with 100% Al dross waste replacing calcined alumina presented statistically

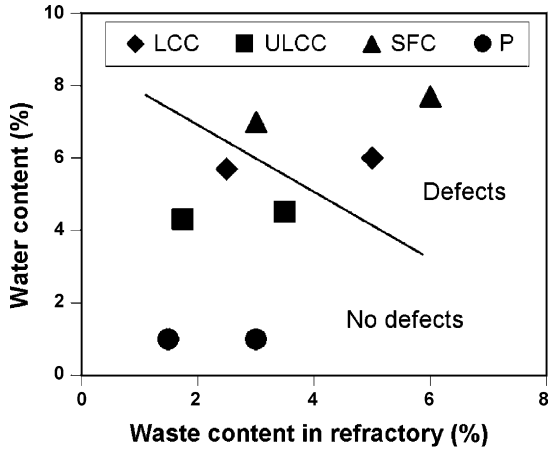

Fig. 9. Water content used to prepare refractory samples plotted as a function of the waste content in refractory (wt% over total mass). The line divides the samples that presented high temperature generated defects and the samples without defects.

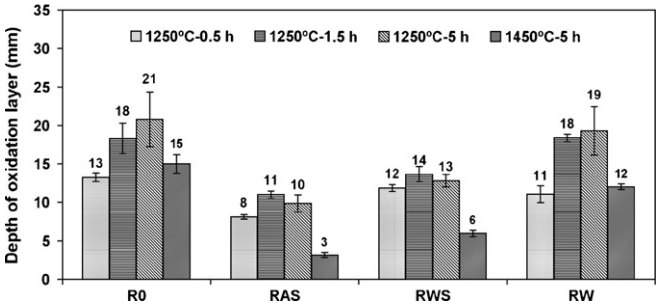

Fig. 10. Results of oxidation resistance test conducted at 1250 °C for 0.5, 1.5, and 5 h and at 1450 °C for 5 h of resin-bonded refractory samples (R): R0 (without anti-oxidant elements), RAS (3.5% Al and 2% Si), RWS (3.5% waste and 2% Si), and RW (5.5% waste).

significant lower value of bulk density after firing at 1450 °C versus control samples (Fig. 6). This change was caused by the expansion of body and increase in porosity (Fig. 8e). The formation of crack-like defects generated by the evaporation of gas at high temperature (Fig. 8c) seems to be the cause of the lowering of the average value of bulk density of the LCC sample with 100% Al dross waste replacing calcined alumina after firing at 1450 °C, although it was not statistically different compared to the result of control sample (at 95% confidence interval, Fig. 4). The mechanical properties (flexural and crushing strengths) evaluated at room temperature of the samples that presented defects generated from firing at 1450 °C (LCC sample with 100% waste replacing calcined alumina, Fig. 4, and SFC samples with 50 and 100% waste, Fig. 6) were not significantly impacted by these defects. In the actual stage of development, however, it seems to be better to avoid the formation of defects, since crack-like defects can increase the stress intensity factor, K_I, at the crack tip [24]. More investigations are necessary to verify the influence of the defects generated at high temperatures on the mechanical reliability of refractories, including high temperature mechanical tests. The results indicate that there are some restrictions related to the type of castable and the waste content in order to avoid the formation of defects (Fig. 8). Fig. 9 indicates the

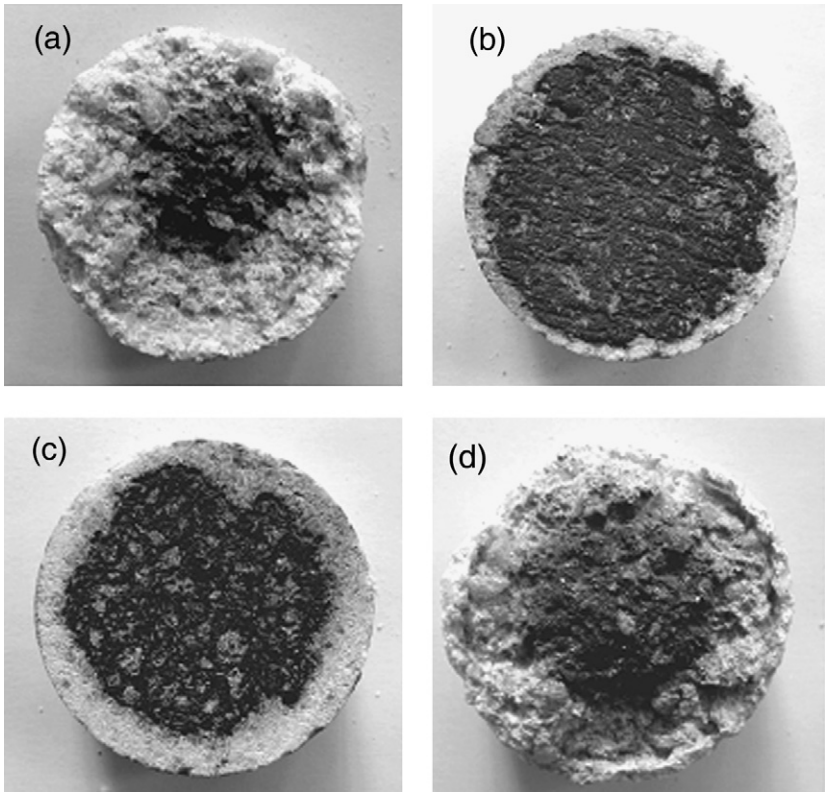

Fig. 11. Cross-sectional view of resin-bonded refractory samples (R) heat-treated in air at 1450 °C for 5 h: (a) R0 (without anti-oxidant elements); (b) RAS (3.5% Al and 2% Si); (c) RWS (3.5% waste and 2% Si); and (d) RW (5.5% waste).

existing relationship between the maximum waste content that can be introduced in a refractory and the maximum water content that can be used during the processing in order to avoid formation of crack-like defects and pores in refractory compositions studied. The maximum water content that can be added decreases with an increase in the waste content. The plot suggests a limit to the waste content that can be introduced in a castable, since the water content necessary for processing the castable increases with the waste content (Fig. 3).

The results of the oxidation resistance test of resin-bonded refractory samples are shown in Fig. 10. In this test, cylindrical specimens (50 mm in diameter and 50 mm in height) were heat-treated at 1250 and 1450 °C in air, with oxidation occurring from the surface to the interior of the specimen (Fig. 11). In Fig. 10, the results of two control samples are shown: R0, without metallic powder and waste; and RAS, with 3.5 wt% Al and 2 wt% Si. As expected, the RAS sample had significantly lower results of oxidation layer thickness versus the R0 sample in all test conditions (at 95% confidence interval). The RWS sample, with 3.5 wt% Al dross waste (substituting Al powder) and 2 wt% Si, presented significant higher results of oxidation layer thickness than RAS sample in all test conditions. In the RW sample, with 5.5 wt% Al dross waste addition (substituting both the Al and Si powders), the results of oxidation layer thickness were also significant higher than the RAS sample in all test conditions, and similar to the results of R0 sample, except after heat treatment at 1250 °C for 0.5 h (at 95% confidence interval). These results showed that Al dross waste did not protect the carbonaceous matrix of resin-bonded refractories against oxidation. The small increases of oxidation layer thickness in the RWS sample compared to the RAS sample indicated that Si powder was more effective than Al powder against oxidation. For all samples, the oxidation was more severe at 1250 °C than at 1450 °C, as observed in another study [25]. XRD results (Fig. 1) indicated that some components in the waste (AlN, CaF_2, and metallic Al) oxidize during high temperature exposition in air. Semi-quantitative analysis by XRD indicated that the total content of these phases in the Al dross waste (before oxidation) was around 33% (Table 5), and that it was mainly AlN. Since the results of oxidation resistance testing (Fig. 10) showed negligible effect of the addition of Al dross waste, it is not expected that the increase in the amount of waste could enhance the oxidation resistance of the carbonaceous matrix of the refractory at a level that would lead to replacement of the anti-oxidant metallic elements (Al and Si). The reason for the weak effect of the dross to protect the carbonaceous matrix seems to be related to the rapid oxidation rate of AlN compound above 1100 °C [26].

3.3. General discussion

Refractories are generally porous materials with a large particle size distribution, which tends to maximize the particle packing density. The large particles (aggregates) form the rigid structure (skeleton), and the fine active particles form the ‘‘matrix’’ of the refractory, which, after firing (sintering), bonds the aggregates. Considering the basic properties evaluated (linear change, bulk density, flexural strength, and cold crushing strength), the results (Figs. 4–7) indicate that Al dross waste from plasma processing can replace fine structural components (calcined alumina and refractory clay) in refractories (castables and bricks), although there are restrictions related to the Al dross waste fraction and processing water content impacting the refractory porosity (Fig. 9). The possibility to use Al dross waste from plasma processing directly, without prior calcination, in refractories is attractive. Although dross as an aggregate can be used in refractories in higher fractions (up to 30 wt%) [17], a high-temperature heat treatment, and possibly a milling operation to adjust the particle size distribution, are necessary to produce this refractory component. The fraction of Al dross waste added to the castable samples (up to ∼5 wt%, Table 1), however, is significant, since the annual consumption of calcined alumina in refractories is around half million metric tonnes [16]. Although the price of refractory clays is lower than the calcined alumina, the use of Al dross waste as replacement for this raw material may be justified by the lower environmental impacts caused by mining. The consumption of refractory clays as fine component is difficult to estimate, since they are also used to produce aggregates for alumina–silica refractories, but it is higher than the consumption of calcined alumina. Therefore, even though the fraction of Al dross waste that can be added directly to the refractory is small (∼5 wt%), the potential market for this material is large.

As mentioned before, plasma processing is a growing technology that has potential to substitute for traditional dross processing, which uses a salt flux to recover Al metal from Al dross. A new advantage of using plasma processing was shown in this work: the waste of this process can be applied directly in refractory materials with minimum costs and operations (deaglomeration and screening). At this moment, it is not know if the capacity of a plasma processing plant will be economically viable, but it will be necessary to evaluate if the volume and type of Al dross waste generated by it is consistent enough as a source of raw materials for refractories.

The compositions investigated were high-alumina refractories (90% or more Al_2O_3, Tables 1 and 4), which are inert to most corrosive fumes and slags, resistant to both reducing and oxidizing atmospheres, exhibit high load bearing ability, and are resistant to spalling, thermal shock, and flame impingement [27]. They can be used in ferrous, non-ferrous, cement, glass, chemical, petroleum, ceramics, and mineral processing industries [27]. The positive results obtained in this work, however, do not validate the use of refractories with additions of Al dross waste for all these applications, since it is important to test critical material properties necessary in each specific application in order to evaluate if the refractory is negatively impacted by the dross additions. These critical properties could include metal or slag resistance.

4. Conclusions

The results of linear change, bulk density, flexural strength at room temperature, and cold crushing strength indicated that Al dross waste from plasma processing may be applied directly,

without prior calcination, as a fine structural components (for calcined alumina and refractory clay) in castables and pressed refractories. The evaluated physical properties are basic and general for most refractories. It will be necessary to test specific material properties like metal and slag resistance, for each specific application in order to evaluate if the refractory is impacted by the dross additions.

The waste content and the water content used in the processing, however, must be optimized in order to avoid the formation of crack-like defects in the microstructure. The gas evolution from the waste, possibly nitrogen and fluorine, generated microstructural defects at high temperature (1450 °C). These defects, however, did not impact the evaluated physical properties. Even though the fraction of Al dross waste that can be added directly to the refractory is small (∼5 wt%), the potential market for this material is large, since the consumption of refractory materials is large.

The waste cannot be used as anti-oxidant component for resin-bonded refractories since it does not protect the carbonaceous matrix against oxidation.

Acknowledgments

The authors would like to acknowledge Dr. A.C. Cruz for the supply of Al dross waste, Mrs. R. Hoshino for the chemical analysis, Mrs. J.L.A. Manholleti for XRD analysis, Dr. L.C. Ferreira (Elfusa Geral de Eletrofusão, Brazil) for the supply of fused aluminas, and Alcoa Alumínio (Brazil), FAPESP, and CNPq for the financial support.

References

[1] O. Manfredi, W. Wuth, I. Bohlinger, Characterizing the physical and chemical properties of aluminum dross, JOM 49 (11) (1997) 48–51.
[2] T. Gens, Recovery of aluminum from dross using the plasma torch, US patent 5,135,565 (1992).
[3] J.A.S. Tenório, D.C.R. Espinosa, Aluminum recycling, in: G.E. Totten, D.S. Mackenzie (Eds.), Handbook of Aluminum: Production and Materials Manufacturing, vol. 2, Marcel Dekker, New York, 2003, pp. 115–153.
[4] T. Hashishin, Y. Kodera, T. Yamamoto, M. Ohyanagi, Z.A. Munir, Synthesis of $(Mg,Si)Al_2O_4$ spinel from aluminum dross, J. Am. Ceram. Soc. 87 (3) (2004) 496–499.
[5] M.C. Shinzato, R. Hypolito, Solid waste from aluminum recycling process: characterization and reuse of its economically valuable constituents, Waste Manage. 25 (2005) 37–46.
[6] I.W. Gower, C.J. Cherry, D.S. Yang, Aluminum dross reclamation, US patent 4,523,949 (1985).
[7] D. Yerushalmi, L. Sarko, Method of recycling aluminum dross, US patent 5,424,260 (1995).
[8] G. Dube, J.-P. Huni, S. Lavoie, W.D. Stevens, Recovery of non-ferrous metals from dross, US patent 4,959,100 (1990).
[9] R.D. Lindsay, Process for recovery of free aluminum from aluminum dross or aluminum scrap using plasma energy with oxygen second stage treatment, US patent 5,447,548 (1995).
[10] M.I. Boulos, New frontiers in thermal plasma processing, Pure Appl. Chem. 68 (5) (1996) 1007–1010.
[11] N. Ünlü, M.G. Drouet, Comparison of salt-free aluminum dross treatment processes, Resour. Conserv. Recycl. 36 (2002) 61–72.
[12] D. Neuschütz, Plasma processing of dusts and residues, Pure Appl. Chem. 68 (5) (1996) 1159–1165.
[13] C. Brisson, G. Chauvette, F.M. Kimmerle, R. Roussel, Process for using dross residues to produce refractory products, US patent 5,132,246 (1992).
[14] R. Breault, S.P. Tremblay, Y. Huard, G. Mathieu, Process for the preparation of calcium aluminates from aluminum dross residues, US patent 5,407,459 (1995).
[15] E.D. Sehnke, Refractory-grade bauxite: an overview—1993, in: Proceedings of the UNITECR, ALAFAR, São Paulo, Brazil, (1993), pp. 658–670.
[16] T.J. Carbone, Production processes, properties, and applications for calcined and high-purity aluminas, in: L.D. Hart (Ed.), Alumina Chemicals: Science and Technology Handbook, The American Ceramic Society, USA, 1990, pp. 99–108.
[17] H.-K. Park, H.-I. Lee, E.-P. Yoon, Process for recycling waste aluminum dross, US patent 6,296,817 B1 (2001).
[18] A.C. Da Cruz, personal communication.
[19] P. Bowen, J.G. Highfield, A. Mocellin, T.A. Ring, Degradation of aluminum nitride powder in an aqueous environment, J. Am. Ceram. Soc. 73 (3) (1990) 724–728.
[20] S. Fukumoto, T. Hookabe, H. Tsubakino, Hydrolysis behavior of aluminum nitride in various solutions, J. Mater. Sci. 35 (2000) 2743–2748.
[21] J.W. Halloran, Calcination, in: Schneider, Jr. (Ed.), Engineered Materials Handbook Ceramics and Glasses, vol. 4, ASM International, USA, 1991, pp. 109–114.
[22] N. Saito, C. Ishizaki, K. Ishizaki, Temperature programmed desorption (TPD) evaluation of aluminum nitride powder surfaces produced by different manufacturing process, J. Ceram. Soc. Jpn. 102 (3) (1994) 301–304.
[23] E.W. Osborne, M.G. Norton, Oxidation of aluminium nitride, J. Mater. Sci. 33 (1998) 3859–3865.
[24] H.N. Yoshimura, P.F. Cesar, W.G. Miranda Jr., C.C. Gonzaga, C.Y. Okada, H. Goldenstein, Fracture toughness of dental porcelains evaluated by IF, SCF, and SEPB methods, J. Am. Ceram. Soc. 88 (6) (2005) 1680–1683.
[25] J. Yu, A. Yamaguchi, Behavior of Al on microstructure and properties of MgO–C–Al refractories, J. Ceram. Soc. Jpn. 101 (4) (1993) 475–479.
[26] H. Fukuyama, T. Tanoue, K. Nagata, Novel process for surface treatment of AlN—high temperature oxidation behavior of AlN, in: Proceedings of the Sixth Pacific Rim Conference on Ceramic and Glass Technology, The American Ceramic Society, 2005.
[27] K.A. Evans, The manufacture of alumina and its use in ceramics and related applications, Key Eng. Mater. 122–124 (1996) 489–526.